A Spectroscopic Analysis of the Phase Evolution in Polyurethane Foams

Amy M. Heintz, Daniel J. Duffy, Chad M. Nelson, Ying Hua, and Shaw L. Hsu*

Polymer Science and Engineering Department, Materials Research Science and Engineering Center, University of Massachusetts (Amherst), Amherst, Massachusetts 01003

Wu Suen and Charles W. Paul

National Starch, Bridgewater, New Jersey 08807

Received July 21, 2005; Revised Manuscript Received August 24, 2005

ABSTRACT: Infrared spectroscopy has been used to study the evolution of polyurethane foam structure, providing measures of relative reaction kinetics, hard segment growth, the onset of phase separation, the formation of order, and the development of final morphology. Changes in free, monodentate, and bidentate hydrogen-bonded urea groups dominate the organization of the entire ensemble. Hard segments formed by reaction of 2,6-toluene diisocyanate (2,6-TDI) and by a mixture of 80% 2,4-TDI and 20% 2,6-TDI displayed very different local segmental alignment, a factor crucial in the development of morphology. Phase separation occurred faster, with fewer and shorter hard segments, in the systems with well-ordered straight chains. The formation and time evolution of monodentate ureas suggest that phase development may be incomplete, or trapped, in systems with ill-defined urea structures. A low degree of spatial order exists in the systems containing these structures.

Introduction

Polyurethanes are one of the most important polymeric materials owing to the flexibility in properties that can be achieved through variations in synthesis and processing conditions. Despite this fact, a detailed understanding of how the developing structure organizes into different phase-separated morphologies is still lacking. Several physical features are known to be influential in affecting the mechanical properties. Generally speaking, the phase-separated morphology is a defining characteristic of polyurethanes. In manufacturing polyurethane foams, the phase-separated morphology evolves during polymerization as a result of the chemical reaction between water and diisocyanate, which yields polyurea oligomers often called hard segments. The hard segments tend to phase separate from the surrounding "soft segments", most often polyethers or polyesters, into hard-segment-rich and hard-segment-poor regions. Hard-segment-rich regions often exhibit spatial order or even crystallinity in some cases and often are referred as domains. Ample data have shown that the size and perfection of hard-segment-rich polyurea domains depend on the composition of the formulation, on the synthetic procedure, and on the temperature profile of the annealing process.[1]

The focus of this study is on understanding how the various chemical structures evolve into these domains and which chemical factors influence that evolution. Many factors need to be considered. The morphology that develops in a given system depends on the competitive reactions that occur. Once formed, the mobility of structural elements (urea oligomers) during this morphological evolution depends on local constraints. In some cases, the polyethers used in many polyurethane formulations have functionality greater than two, and their reaction with diisocyanate yields a chemically cross-linked network. Therefore, phase separation may be effectively halted, depending upon the time that vitrification occurs. The temperature of the sample is also an important factor during synthesis and an important consideration of morphology development. Typical foam is prepared by reacting a diisocyanate with a mixture of water and hydroxyl end-capped polyether. During the reaction between diisocyanate and water, carbon dioxide evolves and serves as the blowing agent. Because of the very exothermic nature of this reaction, the temperature inside the foam is unpredictable, not readily controlled, and may rise to a temperature as high as 140 °C.[2,3]

The structure of the polyurea segments also influences phase behavior. Traditionally, phase separation of reactive polyurethane foams into hard-segment-rich and hard-segment-poor domains is believed to occur due to the chemical incompatibility of soft and hard segments. For example, polyurethane elastomers based on 2,4-tolylene diisocyanate chain extended with a diol do not exhibit phase-separated morphologies, while those chain extended with a diamine do, presumably due to the strong specific interaction of ureas compared to urethanes.[4,5] Analogously, the polyurea hard segments in foams can form stronger hydrogen bonds than the corresponding urethane-containing hard segments found in most elastomers.

On the other hand, it should also be emphasized that specific interactions need not be the only parameter to be considered. In many cases, the excluded-volume effect from the rigid hard segments and their "straightness" may be the dominant factor in inducing phase separation.[6] Phase separation can occur in polyurethane systems even when χ is negative or when no hydrogen bond donor/acceptors are present.[7,8] Molecular simulation studies showed that the volume fraction of hard segments dispersed in the soft phase decreased with an increase in the hard segment length. By considering the similarity between phase separation processes in polyurethanes and liquid crystals, the origin of the phase separation process in polyurethanes can then be considered in terms of the excluded-volume concept. For example, in liquid crystals, oriented anisotropic domains

* To whom correspondence should be addressed: Tel 413-577-1125; Fax 413-545-0082; e-mail slhsu@polysci.umass.edu.

10.1021/ma051599w CCC: $30.25
Published on Web 10/01/2005

Table 1. Polyurethane Formulations Used in This Study

sample	wt % TDI	H_2O/TDI	H_2O/OH
oo-4-22	0.30	0.81	4.42
T80-6-22	0.37	0.82	6.33
T80-4-22	0.30	0.80	4.36
T80-4-40	0.30	0.79	4.30
T80-4-56	0.30	0.77	4.17
T80-4-87	0.30	0.79	4.40
T80-4-113	0.30	0.79	4.35

formed on phase separation are considered a consequence of chain geometry rather than chain−chain interactions.[9] In most polyurethane systems both the enthalpic and entropic contribution should be considered.[6]

Polyurethane chemistry is an interesting but complex process. The kinetics of polyurea formation and the formation of phase-separated structures have not been definitively established. Several experimental studies have examined morphology development in polyurethane foams.[10−15] These studies were concerned with morphology development under adiabatic conditions. Under homogeneous conditions, the molecular weights of polymers formed exhibited a Schultz−Flory distribution.[16,17] Although the volume fraction and the size of hard segments were characterized, those studies did not consider the contribution of kinetics to structural evolution.

In this study, the kinetics of reaction and the development of morphology are studied in situ using infrared spectroscopy. Infrared spectroscopy provides information at a much more localized level than X-ray diffraction. Well-established spectroscopic features[14] are particularly sensitive to changes in hydrogen bonding.[11,18] Foams were prepared under isothermal conditions to control or depress the rate of the cross-linking reaction. Systems based on both 2,6-TDI and T-80 (an 80/20 mixture of 2,4- and 2,6-TDI) were examined. The polyurea segments based on these diisocyanates have very different structures or "straightness". By combining information regarding reaction kinetics with statistical methods, the most probable distribution of structures was determined. The onset, rate, and degree of phase separation and the formation of order in the different polyureas formed by chemical reactions in the evolving foam were studied using specific features in the infrared spectra.

Experimental Section

Materials. The two different diisocyanates employed were 2,6-toluene diisocyanate (Aldrich, 98%) and a mixture of 2,6-toluene diisocyanate (20%) and 2,4-toluene diisocyanate (80%) (T80, Aldrich, tech grade). The polyether used in this study is Voranol 3137 (Dow Chemical Co.). It is a glycerin-initiated poly(propylene oxide) polyether with ∼13% ethylene oxide randomly polymerized into the chain. It is terminated with secondary hydroxyl groups. It has an equivalent weight of 1075 g/mol and an average functionality of 2.79. The catalyst package used in this study is a mixture of Dabco BL-11 (Air Products), Dabco 33-LV (Air Products), and Dabco T-9 (Air Products). Dabco BL-11 is composed of 70% bis(dimethylaminoethyl) ether in a solution of dipropylene glycol. Dabco 33-LV is a solution of 1,4-diazobicyclooctane[19] (33%) in dipropylene glycol. Dabco T-9 is a stannous octanoate. All were used as received.

Foam Preparation. All foams were prepared from 10.00 g of polyether, 0.010 g of Dabco BL-11, 0.020 g of Dabco 33-LV, and 0.014 g of Dabco T-9 with the appropriate amount of water and specific TDI in a plastic beaker. The formulations are shown in Table 1. The general naming scheme is "(TDI type)-(H_2O/OH)-(T_{rxn})". Samples with an "oo" prefix are based on pure 2,6-TDI, while samples with a "T80 prefix" are based on an 80/20 mixture of 2,4-/2,6-TDI. T_{rxn} refers to reaction temperature. The general procedure was as follows: A stock mixture of BL-11 and 33-LV was prepared in a 1:2 ratio by weight and stored in the refrigerator until use. 10.0007 g of Voranol 3137 and 0.0301 g of stock amine catalysts were mixed with a glass rod in a plastic beaker. In separate syringes, 0.3603 g of deionized H_2O and 4.4112 g of T80 were weighed, accounting for the volume that remains in the syringe after ejection. Immediately prior to reaction, 0.0140 g of T-9 was added to the plastic beaker and mixed. H_2O was added via the syringe and stirred vigorously with the glass rod for 2 min, at which point the mixture became clear. Next, specific TDI was added rapidly and again stirred vigorously for 15 s, at which time foaming was observed. A spatula of the foaming mixture was then dropped onto the internal reflecting crystal, as described below in the spectroscopy section. The infrared spectra were then collected. The time interval for each step in the sample preparation and measurement must be well controlled in order to obtain reproducible results.

Scheme 1

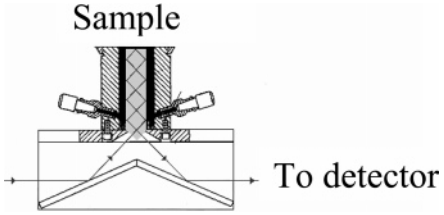

Foaming Kinetics. Infrared spectra were obtained using a Perkin-Elmer 2000 system with a narrow-band MCT detector. Measurements were performed using 4 cm^{-1} spectral resolution. Four scans were signal averaged in order to record time-resolved spectra approximately every 8 s. A nine-pass attenuated total reflectance (ATR) Harrick cell with a ZnSe crystal was used to measure the foaming kinetics, shown in Scheme 1. Sufficient throughput was obtained by applying material to the top of the crystal and leaving the reservoir empty. A heating jacket was used to control the temperature of the crystal. The crystal acted as a heat sink, and the reaction temperature at the foam/crystal interface was controlled in this way. The apparatus was mounted in the N_2-purged sample chamber. Scanning was initiated. Then a droplet of the mixed formulation was allowed to drip from a wedge-shaped spatula onto the crystal. This "dripping" process is important in obtaining reproducible results. Well-defined spectra with stable baseline were obtained. When the reaction was complete, the crystal was soaked in dimethyl sulfoxide, to swells and delaminate the foam.

Analysis of Infrared Spectra. Analysis of the spectra was carried out as described previously.[15] All the bands used in this study are well established in the literature.[20] The set of spectra for each foaming experiment were first normalized to account for differences in contact with the crystal. The integrated CH stretch from 3025 to 2800 cm^{-1} was used to normalize the spectrum. Except for T80-6-22, all formulations contained the same weight fraction of polyether (the main contributor to CH stretch intensity). T80-6-22 contained a lower weight fraction of polyether. Therefore, the intensities of its aromatic, NCO, and urea vibrations were relatively larger.

The NCO conversion was determined from the integrated asymmetric NCO stretch from 2320 to 2050 cm^{-1}. The conversion is defined by

$$P_{\mathrm{NCO}_t} = \frac{[\mathrm{NCO}]_0 - [\mathrm{NCO}]_t}{[\mathrm{NCO}]_0} \quad (1)$$

where $[NCO]_0$ is the integrated intensity of the NCO stretch at zero reaction time. The initial concentration was determined by extrapolating the initial set of data points to $t = 0$.[11,15,18]

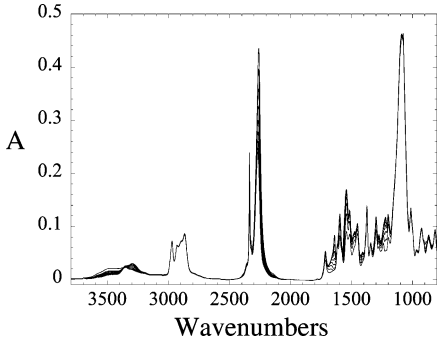

Figure 1. Infrared spectra collected during reaction of T80-6-22. Spectra are shown every 17 s beginning at t_{rxn} = 40 s. Reaction time increases going from black to light gray.

This calculation assumes a second-order reaction kinetics.[21] Additional support for this method is provided by the samples T80-4-T_{rxn}, where T_{rxn} = 22−113 °C. The *y*-intercept in these identical formulations was 35.6 ± 1.4. The deviation from experiment to experiment is small.

Band deconvolution of the amide I region was carried out using the Spectrum 2000 software package. No baseline correction was used. All bands were fit as a mixture of Gaussian and Lorentzian, and the position, bandwidth (bw in cm^{-1}), and intensity were allowed to vary during iteration. For oo-4-22 three bands at 1732 (bw 22−26 cm^{-1}), 1712 (bw 22−26), and 1640 cm^{-1} (bw 11−15) were assumed to be in the 1740−1635 cm^{-1} region. These limits were chosen to avoid changes in the baseline due to contributions from the aromatic C=C ring stretch and amide II bands. It should be noted that 2,4-TDI exhibits a benzene ring stretching frequency at 1617 cm^{-1} whereas 2,6-TDI does not. Therefore, the 1740−1590 cm^{-1} region was analyzed for the T80-based samples. Six bands near 1732 (bw 22−26), 1712 (bw 22−26), 1670−1655 (bw 40−55), 1640 (bw 11−15), 1617 (bw 11−15), and 1596 cm^{-1} (bw 22−26) were analyzed.

Results and Discussion

The influence of hard segment length, structure perfection, and concentration on the phase behavior of reactive polyurethane systems was determined by focusing on three main systems: oo-4-22, T80-6-22, and T80-4-22. Each system was prepared from hydroxyl end-capped polyether, water, diisocyanate, and a catalyst package as discussed in the Experimental Section. Formulations that are similar to those used for commercial slab stock foam were studied. The infrared spectrum obtained during the initial stages of foaming is shown as a function of time for T80-6-22 in Figure 1. Several changes generally occurred for all systems. Reaction with water depleted isocyanate and produced urea groups, while reaction with alcohol from the polyether depleted isocyanate and produced urethane groups. Thus, a decrease in the intensity of the asymmetric NCO stretch between 2050 and 2400 cm^{-1} is observed with simultaneous increases in the intensities of bands due to vibrations associated with various ureas and urethanes. The amide I mode (mainly C=O stretch) between 1600 and 1760 cm^{-1} is the infrared-active vibrational band focused on in this study. Vibrations for urea and urethane groups occur at different frequencies, allowing distinction between the two chemical reactions. The amide I vibration is also very sensitive to the strength and specificity of the hydrogen bonds formed. Generally three types of C=O stretching are found. These are free, hydrogen bonded but not ordered (e.g., monodentate), and hydrogen bonded and highly ordered (e.g., bidentate). Changes in the morphology during

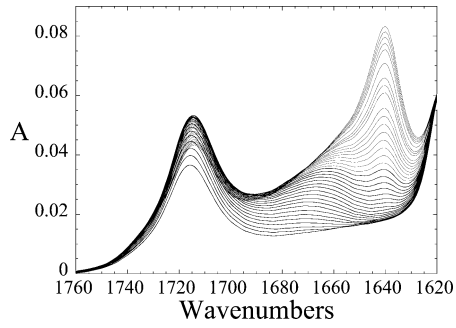

Figure 2. Infrared spectra collected during reaction of T80-6-22 in the amide I region. Spectra are shown every 17 s beginning at t_{rxn} = 40 s. Reaction time increases going from black to light gray traces.

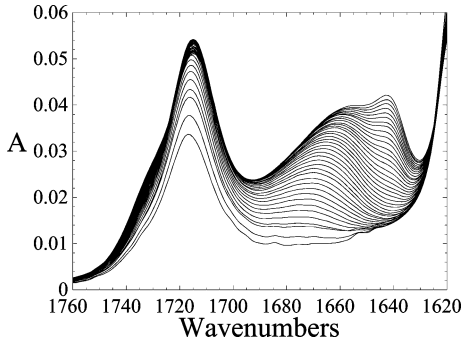

Figure 3. Infrared spectra collected during reaction of T80-4-22 in the amide I region. Spectra are shown every 17 s beginning at t_{rxn} = 30 s. Reaction time increases going from black to light gray traces.

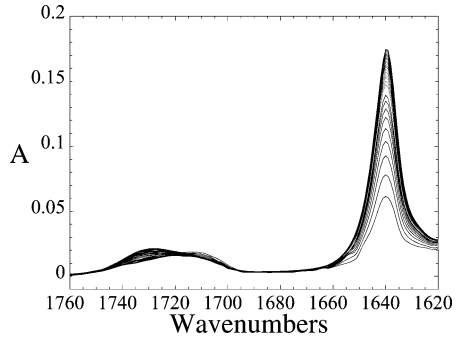

Figure 4. Infrared spectra collected during reaction of oo-4-22 in the amide I region. Spectra are shown every 17 s beginning at t_{rxn} = 45 s. Reaction time increases going from black to light gray traces.

phase separation are then correlated with changes in the hydrogen-bonding characteristics. The band at 1735 cm^{-1} is attributed to free urethane groups, while vibrations at 1715, 1655−1690, and 1640 cm^{-1} are attributed to free, disordered monodentate, and ordered bidentate ureas, respectively. The vibration at 1640 cm^{-1}, in particular, is often used as a characteristic feature of organized hard domains.[22] The amide I region for the three different reacting systems is shown in Figures 2−4.

The time evolution of the infrared spectrum of the oo and T80 systems differ significantly. First, consider the T80-4-22 and T80-6-22 systems. In the early stages of the reaction, the band at 1715 cm^{-1} increases in intensity, as free urea forms. Meanwhile, a broad band near 1670 cm^{-1}, assigned to hydrogen-bonded urea, also increases in intensity. The rate of formation of free urea begins to decrease, however, as a function of time. In

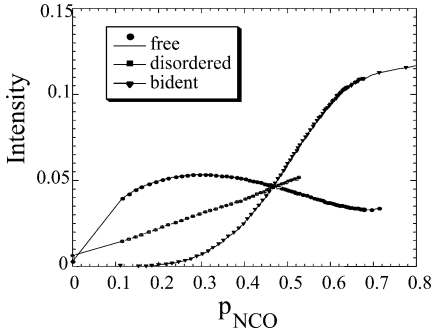

Figure 5. Changes in the band intensity of different types of urea species with increasing reaction conversion for T80-6-22.

contrast, the number of hydrogen-bonded ureas continues to increase. This band shifts about 10 cm^{-1} to lower frequency with increasing conversion, which is associated with the formation of strong hydrogen bonds.[16,17] Finally, at later stages of conversion, a band at 1640 cm^{-1} emerges. This component is assigned to the formation of bidentate urea and is characteristic of ordered hydrogen bonds associated with phase-separated structure. Bidentate urea seems to form at the expense of free urea, which decreases until it reaches a plateau value. For example, a plot of the intensity at 1716, 1665, and 1640 cm^{-1} is shown in Figure 5 for T80-6-22. As conversion is increased, the formation of hydrogen-bonded urea occurs through both depletion of NCO by reaction and depletion of free urea by hydrogen bonding. This behavior is observed for all the systems but is less apparent when the contribution from the overlapping urethane vibration is significant.

The foaming reaction for oo-4-22 exhibits several notable differences from the T80 systems. The formation of bidentate urea was so rapid in this system that a state prior to its formation could not be captured within the time resolution of our infrared instrument. A rise and subsequent depletion of free urea was observed. Monodentate hydrogen-bonded urea was not observed for this system. The morphology is exclusively described by the sharp bidentate urea band at 1640 cm^{-1} and a very small contribution from free urea at 1715 cm^{-1}. The slow formation of urethane, which was difficult to observe in the T-80 system, is apparent at 1732 cm^{-1}.

Characterization of Most Probable Structures. It is clear that the polyurethane foam constituents are highly dependent on the type of diisocyanates used and the structures formed during foam synthesis. To analyze the kinetics data further, differences in the hard segment structures must be considered, specifically in molecular weight and molecular weight distribution and in effective aspect ratio. The degree of polymerization (X) is defined as the number of monomer units per chain, where TDI and water are treated as monomers.[23] This definition is used for convenience. The reactivity and stability of the oligomers formed can differ significantly. The hard segment length and distribution result from the consecutive reaction of diisocyanate and water and terminate when both NCO ends react with polyether hydroxyl groups or when the reactants are depleted. In addition to previous studies,[24−27] the hard segment length and distribution in polyurethane foams have been characterized by mass spectrometry.[28]

Undoubtedly, the hard segment structure and their length distribution are crucial parameters in the formation of phase-separated structures. The symmetric polyurea oligomers formed from pure 2,6-TDI are expected to be more rigid and straight and pack more uniformly than those based upon T-80. The two reactive groups in a difunctional isocyanates show considerable differences in reactivity. Therefore, the molecular weight distribution should then depart from that expected on the basis of equal reactivities. The NCO groups of 2,6-TDI have equivalent reactivity before reaction. But the reactivity of the second NCO group decreases after the first one reacts. The reactivity difference is considerable ($K = k_1/k_2 = 5.32/0.86 = 6.2$).[29]

The polyureas obtained in the T80 system also have different possible structures. The para NCO group of 2,4-TDI is more reactive than the ortho NCO group with a $K = 2.70$ ($k_1 = 11.9$, $k_2 = 4.42$). After reaction between one NCO and water, the reactivity of the ortho group decreases to $k_2 = 1.0$, or $K = 11.9$. Therefore, polyurea segments formed with T-80 should have different sequence distributions than those made from 2,6-TDI alone. It is desirable to obtain a measure of the asymmetry associated with T-80 TDI hard segments. The average sequence length and distribution of 2,6-TDI segments should be related to concentration and reactivity relative to 2,4-TDI. The coupling of 2,4-TDI units in head-to-head or head-to-tail configurations (that is, ureas from para/para, ortho/ortho, or para/ortho coupling) will also depend on the relative reactivities. On the basis of the reactivity and stoichiometry, an example of some of the most probable structures is shown in Scheme 2. The different types of hard segments formed, as expected, is one factor that determines the phase separation kinetics in polyurethanes.

It is also important to examine the possible effects of hard segment length on the polymers formed. The molecular weight distribution of the oligomers formed as a function of NCO conversion can be modeled. A projection of the influence of a change in reactivity on X_w is shown for one of the monomers in Figure 6, where

Scheme 2

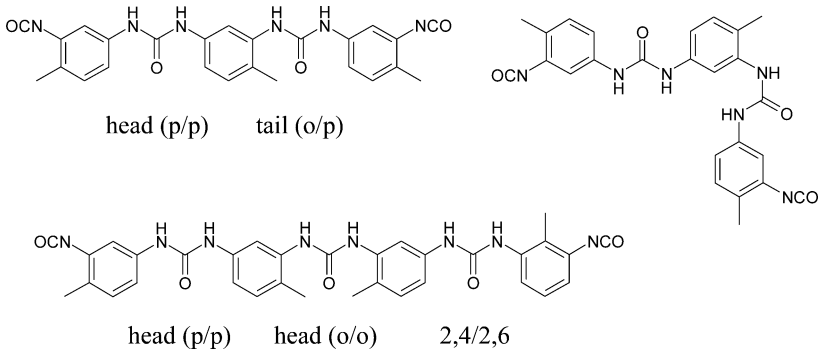

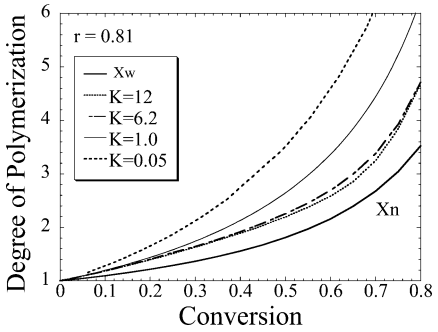

Figure 6. Influence of K on the weight-average degree of polymerization, where K is ratio of the reactivity of a functional group before reaction (k_1) and after one group reacts (k_2). $K = 0.05$ represents water and $K = 6.2$ represents 2,6-TDI.

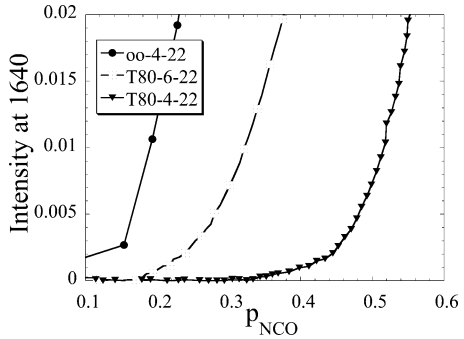

Figure 7. Onset of phase separation for the different foams based on the intensity at 1640 cm^{-1}.

the stoichiometric imbalance parameter r (defined as less than 1 in the theoretical treatment of size distribution) was set equal to 0.81.[30] The effect of the reactivity ratio K is most dramatic at conversion greater than 0.4. In general, a decrease in the reactivity of one functional group upon reaction of the other group ($K > 1$) results in a decrease in the polydispersity. Conversely, an increase in reactivity ($K < 1$) results in an increase in polydispersity. The effect of increasing K from 6.1 to 12 on M_w is very small.[31] Because of the high reactivity of the amine and the stoichiometric excess of NCO, the most abundant species are expected to be odd x-mers with NCO ends. Because of the decrease in reactivity of the second NCO, the TDI monomer should be completely depleted between 75 and 85% conversions. This last prediction is interesting because the reaction between isocyanate and the polyether hydroxyl groups to produce urethane linkages occurs at late conversion.

Onset of Phase Separation. The reacting polyurethane system phase separates due to the structures formed. The importance of contributions from the hard segment length and symmetry (shown in Scheme 2) can be determined by comparing the conversion at the onset of phase separation for the different systems. The growth of bidentate urea, measured by monitoring the intensity at 1640 cm^{-1}, is shown for oo-4-22, T80-6-22, and T80-4-22 in Figure 7. The rapid rise of bidentate urea peak is attributed to phase-separated polyureas. Despite the fact that the stoichiometry of the oo-4-22 and T80-4-22 systems is identical, the oo-4-22 TDI phase separates at a much lower conversion. This cannot be attributed to differences in the average molecular weight and must be associated with differences in either the aspect ratio or the specific hydrogen-bonding interactions.

The onset of phase separation based on changing spectroscopic features is related to changes in the local

Table 2. Onset of Phase Separation Found for Different Polyurethane Samples

sample	p_{NCO}	p_{H_2O}	X_n
oo-4-22	0.10	0.12	1.12
T80-6-22	0.19	0.23	1.26
T80-4-22	0.28	0.35	1.46
T80-4-40	0.28	0.35	1.45
T80-4-56	0.27	0.35	1.44
T80-4-87	0.23	0.29	1.34
T80-4-113	0.26	0.33	1.41

aggregation, which is not necessarily correlated with the structural formation that would be detected using other methods, such as diffraction. Spectroscopic methods are used for analyzing structural elements that are much more localized than those to which other techniques are sensitive. Here the onset of phase separation is taken as the point at which 1640 cm^{-1} band is first observed. The onset occurs near 10% and 28% conversion for the oo-4-22 and T80-4-22 systems, respectively. When the concentration of TDI is increased from 30% in T80-4-22 to 37% in T80-6-22, the onset of phase separation occurs at 19% conversion.

Assuming the conversion due to urethane formation is negligible, X_n at onset can be determined as shown in Table 2. Accounting for the fact that $p_{H_2O} = p_{NCO}/r$, X_n at onset is predicted to be 1.12, 1.26, and 1.46 for oo-4-22, T80-6-22, and T80-4-22, respectively. While this value is quite low, it does not suggest that the formation of dimer is sufficient to cause phase separation. Even at low concentration, the larger oligomers are very influential, as suggested by the tremendous effect of increasing the TDI concentration from 30% in T80-4-22 to 37% in T80-6-22. Flory calculated the minimum X_n required to induce phase separation in a polydisperse mixture of noninteracting rods.[32] The value 2.3 is higher than that found here. This suggests that interchain interaction must also be a contributing factor in the phase separation behavior in this system.

The foam formulation of T80-4-22 was also used to characterize reaction kinetics at temperatures ranging from 40 to 113 °C. In systems in which hydrogen bonding is important, the interaction parameters should depend on temperature.[33] The growth of bidentate urea for different reaction temperatures is shown in Figure 8. The conversion reflects both conversion to urea and conversion to urethane. The average hard segment length is related only to the urea concentration. The ratio of the urea to urethane kinetics is not constant with temperature due to the catalyst package used here. However, only for the samples prepared at 87 and 113 °C (T80-4-87 and T80-4-113) is there any appreciable amount of urethane formed prior to 50% conversion. As shown in Figure 8, the temperature has little or no effect on the onset of phase separation. The formation of bidentate urea is influenced by temperature somewhat, however. The rate of growth is fastest for the sample prepared at 87 °C.

Degree of Phase Separation. The development of morphology as a function of time is reflected in changes in the hydrogen bonding. The data shown in Figure 5 for T80-6-22 can be understood more clearly if the spectra are first deconvoluted into the different contributions from urethane and free and hydrogen bonded urea, as described in the Experimental Section. The relative populations can then be calculated on the basis of band areas rather than band maxima. The absorption coefficients for the different bands are not the same, and

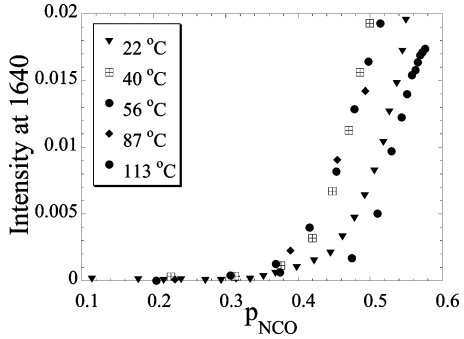

Figure 8. Influence of temperature on the onset of phase separation for T80-4.

thus band deconvolution does not give quantitative results.[34] Nevertheless, this method allows a separation of overlapping bands, such as the monodentate and bidentate hydrogen bonds. The results are shown in Figure 9a−c for samples oo-4-22, T80-6-22, and T80-4-22, respectively.

The difference between the oo and T80 samples is striking. As mentioned above, the morphology of oo-4-22 is described exclusively by free and bidentate urea. The initial growth of bidentate urea is accompanied by a depletion of free urea. After 200 s, the growth of bidentate urea begins to plateau, and accordingly, the free urea begins to increase again. It is shown in Figure 9a, and is evident in Figure 4, that the interference of urethane at long reaction times makes an accurate analysis of the free urea band difficult to achieve. Nevertheless, this analysis yields a qualitative assessment of the structural composition.

The T80-6-22 and T80-4-22 systems are similar. The stoichiometry of T80-6-22 gives fewer urethane linkages, making this sample easier to study. The infrared active bands can be deconvoluted with greater confidence. Both samples are composed of free and bidentate urea and display a broad monodentate hydrogen-bonded urea. The latter band is composed of an ensemble of different hydrogen-bonded conformations of a variety of geometries and strengths. As in oo-4-22, the growth of bidentate urea in the T80-6-22 sample shown in Figure 9b is accompanied by a depletion in free urea content. As the bidentate growth reaches a plateau, the amount of free urea reaches a minimum. The monodentate hydrogen bonds also show an initial increase followed by a decrease. However, in contrast to the free ureas, the depletion of monodentate hydrogen bonds does not occur until after a sufficient population of bidentate urea has formed. The decrease in the area of the monodentate hydrogen bonds occurs due to a narrowing of the bandwidth, shown in Figure 2. Both the narrowing and accompanying band shift indicates a change in the ensemble toward a more ordered state.

The organization of the monodentate hydrogen bonds shown in Figure 9c occurs even before the appearance of bidentate ureas in T80-4-22. The changes in the band contour are similar to those in T80-6-22, but the formation of bidentate urea is much slower. There is an increase in intensity at 1640 cm^{-1}, but no appreciable band is observed. The point taken as the onset of phase separation corresponds to the decrease in free urea content. The time scale to reach a plateau value is approximately 2500 and 5000 s for T80-6-22 and T80-4-22, respectively. It should be noted that T80-6-22 contains a higher concentration of urea groups, so the absolute areas cannot be directly compared.

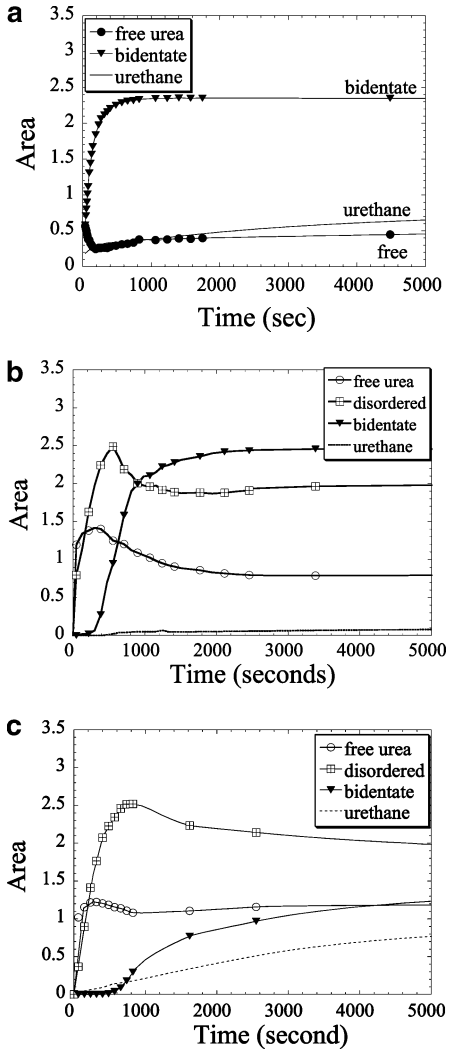

Figure 9. Changes in hydrogen bonding with time during reaction and phase separation as determined by band deconvolution: (a) oo-4-22; (b) T80-6-22; (c) T80-4-22.

Table 3. Degree of Phase Separation Found for Different Polyurethane Samples

sample	free (%)	bidentate (%)
oo-4-22	11	89
T80-6-22	15	47
T80-4-22	30	30

By neglecting the differences in absorption coefficient for free and hydrogen-bonded species,[34,35] the fraction of free and bidentate urea can be approximated from the area of the three bands, as shown in Table 3. The free urea is often referred to as "soluble" urea and, presumably, is only found in the hard-segment-poor domains. On the basis of spectroscopic evidence, the relative amount of urea that remains in the this phase is 11, 15, and 30% for oo-4-22, T80-6-22, and T80-4-22, respectively. Bidentate urea corresponds to a very specific geometry and is overwhelmingly found in the ordered hard-segment-rich domains. If this amount is taken as being related to the degree of phase separation, the relative amount of urea that is found in hard-segment-rich domain is 89, 47, and 30% for oo-4-22, T80-6-22, and T80-4-22, respectively. The difference between the two sets of values is related to the location of monodentate urea, which can be in either the phase mixed or phase-separated state.

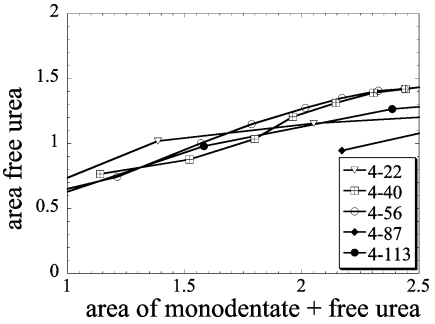

Figure 10. Influence of temperature on changes in hydrogen bonding prior to the formation of bidentate urea as determined by band deconvolution.

The observation of hydrogen-bonded monodentate urea is not unusual. Hydrogen-bonded monodentate urea can exist in the absence of a phase-separated morphology. Under equilibrium conditions, the number of free and hydrogen-bonded ureas should depend on temperature and thus reaction temperature. Prior to the formation of bidentate urea, a plot of free urea vs total urea is virtually independent of temperature, as shown in Figure 10. For reaction temperatures between 22 and 87 °C, the amount of free urea appears to reach a similar plateau value from 30 to 32%. The sample prepared at 113 °C contains a larger amount of free urea, 40%. These results suggest that the amount of monodentate urea observed is due to the slower kinetics at lower reaction temperatures.

Development of Morphology from Reacting Structural Elements. It is now possible to develop a model showing how the reacting system evolves into a phase-separated morphology.[6] For oo-4-22, the initial formulation containing 2,6-TDI, water, and polyether reacts and ureas begin to form. After 12% of the water has been converted to urea, the system begins to phase separate. This occurs through association of longer polyurea segments into ordered bidentate urea. The reaction between water and NCO continues to occur during phase separation. Each new urea is immediately converted into a bidentate urea. This suggests that even the lowest molecular weight oligomers are effectively partitioned to the hard-segment-rich domain upon formation.

For the T80 systems, an increasing concentration of free urea during reaction causes association of the ureas into monodentate hydrogen bonds. This may indicate the initial stages of phase separation for this system, which occurs much more slowly than in oo-4-22. As reaction continues, the concentration of free and hydrogen-bonded urea increases, and the geometry and strength of the hydrogen bonds improve. The formation of bidentate urea occurs at a much later stage. In the initial stages, spatial ordering occurs through depletion of free polyurea segments. In later stages, monodentate hydrogen-bonded urea is also depleted, i.e., reorganized. In the T80 systems, further reaction between the water and isocyanate leads to an increase in hydrogen-bonded structures. The free urea reaches a plateau, which suggests that the phase separation is complete. However, the "slowness" of the morphology development indicated by changes in the monodentate hydrogen bonds suggests a morphology that is not fully evolved. The spatial ordering may not be complete or in a preferred state. Despite the fact that the concentration of TDI is the same for oo-4-22 and T80-4-22, different morphological features exist. Such behavior is interesting considering that the morphology of polyurethanes is often described as consisting of either isolated domains or interconnected domains.[36]

The "ordered structure" of the oo-4-22 hard segments influences all aspects of morphology development. In particular, this system exhibits substantial structural order. Evidence in the literature suggests that hydrogen-bonding interactions are stronger with the para urea of 2,4-TDI than with the ortho urea of 2,6-TDI.[4] The temperature was also found to have little effect on phase separation when chemical cross-linking was absent. Thus, it is unlikely that hydrogen-bonding interactions are the dominant driving force for phase separation. While hydrogen bonds will stabilize the hard domains, the difference in excluded volume between the oo and the T80 hard segments seems to be more important. In addition, the structural irregularity of the T80 hard segments, due to various head−head and head−tail linkages, inhibits spatial ordering. It would be interesting to observe the morphology development of rigid, yet structurally irregular rods.

Conclusions

The phase evolution of reacting polyurethane foams was studied in situ using infrared spectroscopy. The influence of structural irregularity in the hard segments was studied using systems based on 2,6-TDI or an 80/20 mixture of 2,4-/2,6-TDI. Both the chemical reaction and the development of morphology were studied using infrared features specific to different chemical functional groups and to hydrogen bonding.

The onset of phase separation occurred at much lower conversion for the sample based on 2,6-TDI. Increasing the concentration of TDI was also found to decrease the onset time. The number-average hard segment length (X_n) at the onset of phase separation was 1.12 and 1.46 for formulations based on 2,6-TDI and on 80/20 2,4-/2−6-TDI, respectively. These values are lower than predicted by Flory's theory for noninteracting rods, demonstrating the importance of both excluded-volume effect and specific intermolecular interactions. The temperature was found to have very little effect on the onset of phase separation.

The changes in the fraction of free and hydrogen-bonded urea groups as a function of time were used to study the development of morphology. The phase-separated morphology of polyurethane with 2,6-TDI hard segments develops very rapidly through the conversion of soluble free urea into bidentate hydrogen-bonded urea. New urea groups, formed from further reaction, are directly incorporated into the hard domains. The amount of free urea reaches a plateau value near 11%, suggesting complete phase separation. These materials exhibit a high degree of spatial order.

On the other hand, polyurethanes with hard segments based on 80/20 2,4-/2,6-TDI phase separate at a slower rate, although the rate is slightly enhanced by increasing the concentration of TDI. A high concentration of monodentate hydrogen bonds forms prior to the formation of bidentate urea. The fraction of these monodentate hydrogen bonds formed during reaction is nearly independent of temperature. The data suggests that the monodentate hydrogen bonds characterize a phase separating, but spatially disordered, state. The monodentate hydrogen bonds organize with increasing conversion and as phase separation ensues. The amount

of free urea reaches a plateau near 15 or 30%, depending on the concentration of TDI. However, the degree of spatial order, represented by the fraction of bidentate urea, is much lower than in the structurally regular system.

References and Notes

(1) Yontz, D. J. In *Polymer Science and Engineering Department*; University of Massachusetts: Amherst, MA, 1999; p 329.
(2) Gheluwe, P. V.; Leroux, J. *J. Appl. Polym. Sci.* **1983**, *28*, 2053−2067.
(3) Yontz, D. J.; Hsu, S. L.; Lidy, W. A.; Gier, D. R.; Mazor, M. H. *J. Polym. Sci., Polym. Phys.* **1998**, *36*, 3065−3077.
(4) Paik Sung, C. S.; Schneider, N. S. *Macromolecules* **1975**, *8*, 68−73.
(5) Paik Sung, C. S.; Smith, T. W.; Sung, N. H. *Macromolecules* **1980**, *13*, 117−121.
(6) Tao, H. J.; Fan, C. F.; MacKnight, W. J.; Hsu, S. L. *Macromolecules* **1994**, *27*, 1720.
(7) Harrell, L. L., Jr. *Macromolecules* **1969**, *2*, 607−612.
(8) Kornfield, J. A.; Spiess, H. W.; Nefzger, H.; Eisenbach, C. D. *Macromolecules* **1991**, *24*, 4787−4795.
(9) Flory, P. J. *Proc. R. Soc. London* **1956**, *A234*, 73.
(10) Rossmy, G.; Lidy, W.; Schator, H.; Wiemann, M.; Kollmeier, H. J. *J. Cell. Plast.* **1979**, *15*, 276−280.
(11) Artavia, L. D.; Macosko, C. W. *J. Cell. Plast.* **1990**, *26*, 490−511.
(12) McClusky, J. V.; Priester, R. D., Jr.; O'Neill, R. E.; Willkomm, W. R.; Heaney, M. D.; Capel, M. A. *J. Cell. Plast.* **1994**, *30*, 338−360.
(13) Elwell, M. J.; Mortimer, S.; Ryan, A. J. *Macromolecues* **1994**, *27*, 5428−5439.
(14) Elwell, M. J.; Ryan, A. J.; Grunbauer, H. J. M.; Van Lieshout, H. C. *Macromolecules* **1996**, *29*, 2960−2968.
(15) Elwell, M. J.; Ryan, A. J.; Grunbauer, H. J. M.; Van Lieshout, H. C. *Polymer* **1996**, *37*, 1353−1361.
(16) Heintz, A. M. In *Polymer Science and Engineering Department*; University of Massachusett: Amherst, MA, 2003.
(17) Duffy, D. J.; Heintz, A. M.; Stidham, H. D.; Hsu, S. L.; Suen, W.; Chu, W.; Paul, C. W. *J. Adhes.* **2003**, *79*, 1091−1107.
(18) Priester, R. D.; McClusky, J. V.; O'Neill, R. E.; Harthcock, M. A.; Davis, B. L. *33rd Annual Polyurethane Technical/Marketing Conference 1990*, *Sept 30−Oct 3*, pp 527−538.
(19) University of Massachusetts (Lowell), 2000.
(20) Dehaseth, J. A.; Andrews, J. E.; McClusky, J. V.; Priester, R. D.; Harthcock, M. A.; Davis, B. L. *Appl. Spectrosc.* **1993**, *47*, 173−179.
(21) Satchell, D. P. N. S. R. S. *Chem. Soc. Rev.* **1971**, 231−250.
(22) Miyazawa, T.; Blout, E. R. *J. Am. Chem. Soc.* **1961**, *83*, 712−719.
(23) Heintz, A. M.; Duffy, D. J.; Hsu, S. L.; Suen, W.; Chu, W.; Paul, C. W. *Macromolecules* **2003**, *36*, 2695−2704.
(24) Castro, J. M.; Lopez-Serrano, F.; Camargo, R. E.; Macosko, C. W.; Tirrell, M. *J. Appl. Polym. Sci*. **1981**, *26*, 2067−2076.
(25) Peebles, L. H., Jr. *Macromolecules* **1976**, *9*, 58−61.
(26) Krol, P. *Polimery* **1997**, *42*, 458−464.
(27) Barreiro, M. F.; Dias, R. C. S.; Costa, M. R. N. *Macromolecules* **1994**, *27*, 7650−7653.
(28) Yontz, D. J.; Hsu, S. L. *Macromolecules* **2000**, *33*, 8415−8420.
(29) Brock, F. H. *J. Org. Chem.* **1959**, *24*, 1802−1804.
(30) Gandhi, S. S.; Gibson, M. S.; Kaldas, M. L.; Vines, S. M. *J. Org. Chem.* **1979**, *44*, 4705−4707.
(31) Peebles, L. H., Jr. *Macromolecules* **1974**, *7*, 872−882.
(32) Flory, P. J. *Macromolecules* **1978**, *11*, 1141.
(33) Painter, P. C.; Shenoy, S. L.; Bhagwagar, D. E.; Fishburn, J.; Coleman, M. M. *Macromolecules* **1991**, *24*, 5623−5629.
(34) Brozoski, B. A.; Painter, P. C.; Coleman, M. M. *Macromolecules* **1984**, *17*, 1591−1594.
(35) Lee, H. S.; Wang, Y. K.; Hsu, S. L. *Macromolecules* **1987**, *20*, 2089−2095.
(36) Aneja, A.; Wilkes, G. L. *J. Appl. Polym. Sci.* **2002**, *85*, 2956−2967.

MA051599W